

## **miR-126 Orchestrates an Oncogenic Program in B-Cell Precursor Acute Lymphoblastic Leukemia**

Silvia Nucera<sup>1,7</sup>, Alice Giustacchini<sup>1,2,7</sup>, Francesco Boccalatte<sup>1,2,7</sup>, Andrea Calabria<sup>1</sup>,  
Cristiana Fanciullo<sup>1,2</sup>, Tiziana Plati<sup>1</sup>, Anna Ranghetti<sup>1</sup>, Jose Garcia-Manteiga<sup>3</sup>, Davide  
Cittaro<sup>3</sup>, Fabrizio Benedicenti<sup>1</sup>, Eric R Lechman<sup>4</sup>, John E. Dick<sup>4</sup>, Maurilio Ponzoni<sup>2,5</sup>,  
Fabio Ciceri<sup>2,6</sup>, Eugenio Montini<sup>1</sup>, Bernhard Gentner<sup>1,6,8</sup> and Luigi Naldini<sup>1,2,8</sup>

<sup>7</sup> Co-first author

<sup>8</sup> Co-senior author

<sup>1</sup>San Raffaele Telethon Institute for Gene Therapy, <sup>2</sup>Vita Salute San Raffaele University, <sup>3</sup>Centre for Translational Genomics and Bioinformatics, <sup>4</sup>Princess Margaret Cancer Centre, University Health Network, Toronto and Dept. of Molecular Genetics, University of Toronto, Canada, <sup>5</sup>Pathology Unit, <sup>6</sup>Hematology and Bone Marrow Transplantation Unit, IRCSS Ospedale San Raffaele, Milano, Italy

Correspondence: [gentner.bernhard@hsr.it](mailto:gentner.bernhard@hsr.it) (B.G.), [naldini.luigi@hsr.it](mailto:naldini.luigi@hsr.it) (L.N.)

## SUMMARY

MicroRNA-126 is a known regulator of hematopoietic stem cell quiescence. We engineered murine hematopoiesis to express miR-126 across all differentiation stages. Thirty percent of mice developed monoclonal B-cell leukemia, which was prevented or regressed when a tetracycline-repressible miR-126 cassette was switched off. Regression was accompanied by up-regulation of cell cycle regulators and B-cell differentiation genes, and down-regulation of oncogenic signaling pathways. Expression of dominant-negative p53 delayed blast clearance upon miR-126 switch-off, highlighting the relevance of p53 inhibition in miR-126 addiction. Forced miR-126 expression in mouse and human progenitors reduced p53 transcriptional activity through regulation of multiple p53-related targets. miR-126 is highly expressed in a subset of human B-ALL, and antagonizing miR-126 in ALL xenograft models triggered apoptosis and reduced disease burden.

## SIGNIFICANCE

Several lines of evidence link stem cell gene expression programs with cancer. Here we show that miR-126, a regulator of HSC quiescence, causes leukemia in mice if not physiologically down-regulated during early steps of differentiation. The diseases strictly depend on sustained miR-126 expression. Likewise, we found evidence for miR-126 dependence in human B-ALL. We show that miR-126 orchestrates an oncogenic program in B-ALL by down-regulating p53-dependent pathways enabling evasion of senescence, cell cycle arrest and apoptosis, and maintaining blasts in a proliferative B-cell precursor state. Because it reproduces human B-ALL hallmarks, our model will help investigating pathogenesis and therapeutic strategies. Targeting of miR-126 or its downstream pathways offers the prospect to deplete leukemic cells while expanding normal HSC.

## INTRODUCTION

The importance of microRNAs (miR) as posttranscriptional regulators of gene expression has been widely established (Bartel, 2009). miRs regulate multiple targets within the same or functionally linked pathways thus integrating compound signals into a functional outcome that can be tissue- and cell-type specific. In the hematopoietic system, miRs affect multiple processes including hematopoietic stem cell (HSC) maintenance and activation, lineage choice, differentiation and immune cell function (Gruber et al., 2009; Guo et al., 2010). Deregulated miR activity can contribute to hematologic malignancy: miR-15~16 and the miR-34 family are well established tumor suppressor miRs lost in chronic lymphocytic leukemia (CLL) and other lymphoid malignancies (Blandino et al., 2014), while miR-145 and 146a are deleted in the 5q- syndrome (Starczynowski et al., 2010). On the other hand, several miRs have been shown to induce hematologic malignancy upon forced expression in mouse hematopoietic cells, namely miR-155 (O'Connell et al., 2008), miR-125a/b (Bousquet et al., 2010; Guo et al., 2012), miR-29a (Han et al., 2010), members of the miR-17~92 cluster (He et al., 2005; Xiao et al., 2008) and miR-21 (Medina et al., 2010). Several of these oncomiRs are also expressed in HSC where they regulate stem cell functions (Guo et al., 2010; Ooi et al., 2010), and, when artificially expressed, they are often capable of inducing both myeloid and B-cell tumors, depending on the promoter used to drive miR over-expression. A link between active stem cell programs and cancer-initiating capacity has been established for diseases with a stem cell hierarchy, such as acute myeloid leukemia (Eppert et al., 2011), so it is plausible that HSC miRs fulfill a similar role in this context as well. We have recently identified miR-126 as an HSC regulator, with highest expression levels found in the most primitive HSC and down-regulation occurring at the stage of lineage-committed progenitors (Gentner et al., 2010; Chiriaco et al., 2014). We previously showed that miR-126 attenuates PI3K/AKT signaling restraining HSC activation and cell cycle entry (Lechman et al., 2012). Stable miR-126 inhibition expanded murine and human HSC *in vivo* without leading to their exhaustion or transformation in spite of activated PI3K/AKT signaling. Conversely, stable miR-126 overexpression (126/OE) increased HSC quiescence *in vivo* leading to a progressively lower contribution to hematopoietic output. However, miR-126/OE expression resulted in increased proliferation of progenitor cells and enhanced short-term repopulation post

transplantation, a phenomenon that was particularly evident in the B-cell lineage. Thus, HSC and progenitors responded differently to 126/OE, pointing to a context-specific effect of this miR. The mechanistic basis of the differential response and the long-term consequences of 126/OE on progenitor cell biology remain to be determined, as well as the role of miR-126 in hematologic malignancies. We here shed light on these questions by overexpressing miR-126 in mouse hematopoietic stem and progenitor cells (HSPC) establishing a link between this stem cell miR and B-cell acute lymphoblastic leukemia, a disease which is, in general, not characterized by a stem cell hierarchy.

## RESULTS

### Forced miR-126 expression in mouse hematopoietic stem and progenitor cells is oncogenic

During long-term follow up of mice transplanted with Lineage (Lin)<sup>-</sup> HSPC transduced with lentiviral vectors (LV) constitutively expressing miR-126 (SFFV-126/OE, Figure 1A), we found that a substantial fraction of mice in the 126/OE group (16/57 mice in 6 independent experiments) developed leukemia with a median latency of 27 weeks (range: 13-38 weeks), while none of the control LV-transduced mice did (n=36). Incidence reached up to 60% in the experiments with longest follow-up and highest transduced cell chimerism (Figure 1A). Leukemia occurrence was preceded by the transient appearance of an abnormal population of CD19<sup>+</sup> cells with an immature, CD45<sup>low</sup>Immunoglobulin(Ig)M<sup>+</sup>IgD<sup>-</sup> phenotype in the peripheral blood (PB) (Figure 1B). Bone marrow (BM) analysis of leukemia-free 126/OE mice at different time-points showed an increased number of early B-cell differentiation stages with a concomitant decrease in mature B-cells pointing to a delay or partial differentiation block induced by 126/OE (Figures S1A-C). Moreover, OFP<sup>+</sup> B-cell precursors from the 126/OE group of mice showed decreased levels of apoptosis (Figure S1D). Whereas the abnormal B-cell population generally disappeared after stabilization of post-transplant hematopoiesis, some mice showed persistence or re-appearance of immature B-cells in the PB, which progressively expanded (Figure 1C). Mice became severely ill manifesting progressive anemia, thrombocytopenia, hyperleukocytosis or leukocytopenia with evidence of blasts in the blood smear (Figures 1D-E), as well as signs of distress. Splenomegaly, lymphadenopathy, the presence of bulky tumor masses and macroscopic organ infiltrations were common necropsy findings. Histopathology confirmed heavy infiltration of the BM, lymph nodes and several organs by small to intermediate sized blast cells with a high mitotic index resulting in a disruption of the normal cellular architecture (Figures 1F and S2). All tumors were of hematopoietic origin (CD45<sup>dim/+</sup>) and expressed the 126/OE vector ( $\geq 90\%$  OFP<sup>bright</sup>) (Figure 1G). Most of the tumors (75%) could be classified as high-grade precursor B-cell neoplasms, with a CD19<sup>+</sup>B220<sup>+</sup>IgM<sup>-</sup> immunophenotype on FACS (Figures 1G and S1E) and B220<sup>+</sup>CD3<sup>-</sup>Bcl6<sup>+</sup>Mum1<sup>+</sup> on immunohistochemistry (Figure S2A). Blasts generally showed nonproductive, monoclonal rearrangements of

the Ig heavy chain locus (Figure S1F and Table S1). Moreover, most diseases co-expressed a primitive progenitor surface antigen such as c-Kit and/or Sca-1 and contained a variable proportion of CD11b<sup>+</sup> cells (Figures 1G and S1E). Four out of 16 studied tumors (25%) showed an immature myeloid phenotype (CD11b<sup>+</sup>CD19<sup>-</sup>) with high expression of c-Kit, absence of Ig locus rearrangements (mouse H0) and negativity for myeloperoxidase staining (mouse A2) (Figure S2B and Table S1).

We also performed a comprehensive analysis of lentiviral integration sites (IS) on purified leukemia cells and distinct hematopoietic lineages from both leukemic and pre-leukemic mice (Figures 1H and S3 and Table S2). These studies further indicate that tumors are monoclonal (Figure S3C-D) and, because IS retrieved from leukemic cells were not preferentially found near oncogenes but rather near different genes in different tumors, provide no evidence for insertional mutagenesis as a mechanism of transformation (Figures S3A-B). We then exploited the unique IS retrieved from n=6 diseases as genetic markers to backtrack their origin from pre-leukemic clones on prospectively banked PB leukocyte subpopulations. Disease-specific IS were detectable up to 5 months before leukemia onset and occurred in multiple lineages in 4/6 mice, while they were mostly limited to B-cells in 2 mice (mouse B1&C1, Figures 1H and S3E), arguing in favor of a multipotent progenitor cell origin in the majority of cases. Moreover, disease-specific IS were highly represented in the abnormal CD19<sup>+</sup>OFP<sup>+</sup>CD45<sup>low</sup> B-cell population molecularly proving its clonal relationship with the leukemia and supporting its role as a precursor lesion (Figures 1H and S3E).

In summary, forced miR-126 expression in HSPC increased the number of B-cell progenitors reducing apoptotic rate and delaying their differentiation into mature B-cells. These events eventually led to development of monoclonal leukemia, predominantly of B-cell precursor phenotype, with a latency of 3 to 9 months and a penetrance of up to 60%.

### **Withdrawal of ectopically expressed miR-126 induces leukemia regression**

To establish whether constitutive expression of miR-126 is critical for the induction and maintenance of leukemia, we transduced Lin- cells with a Tetracycline regulated system (Tet.126), which allows turning ectopically expressed miR-126 off by Doxycycline (Doxy) administration (Figure 2A). After validation of the system (Figures S4A-B), we transplanted mice with Tet.126-transduced HSPC. As with

constitutive 126/OE, mice released immature  $CD19^+CD45^{\text{low}}$  B-cells into the PB, which was accompanied by a maturation block and reduced apoptosis in BM B-cell precursors at 4 weeks post-transplant (Figure S4C). We then performed secondary transplantation, injecting equal amounts of BM cells from one donor into two recipient mice thus establishing paired grafts (Figure 2A). Three weeks after transplantation, we treated a mouse from each pair (n=11) preemptively with Doxy (Doxyl<sup>PE</sup>) and compared the abnormal B-cell population in the blood to the matched untreated mouse. Doxy<sup>PE</sup> administration rapidly turned the vector cassette off (as shown by OFP down-regulation) and induced the disappearance of  $CD19^+CD45^{\text{low}}$  immature B-cells within 5 days, further supporting the notion that these cells appear as a direct consequence of forced miR-126 expression (Figure 2B). During follow-up, 5/14 mice in the no-Doxy group developed B-cell neoplasia that showed similar characteristics as the SFFV-126/OE-induced tumors, while no tumors were detected in the 11 matched mice from the Doxy<sup>PE</sup> group (Figure 2C). In summary, the development of B-cell malignancy was effectively prevented by turning the miR-126 vector cassette off during the pre-leukemic stage of the disease, and mice remained tumor-free >4 months after discontinuation of Doxy treatment.

Next, we investigated whether silencing of the miR-126 vector cassette could control established leukemia (Figures 2D-F). In a first set of experiments, we transplanted the BM from 2 cases of B-cell leukemia into healthy recipients (n=4 recipients per disease; disease #2: sublethally irradiated recipients; disease #11: no conditioning). Half of the mice prophylactically received Doxy at the time of transplant (Doxyl<sup>proph</sup>), while the other half was kept Doxy-free until they manifested leukemia. None of the 4 Doxy<sup>proph</sup> mice developed B-cell leukemia over a median follow up of 5 months, even when Doxy treatment was suspended for several months. On the contrary, the mice that received the paired graft and were kept off Doxy developed B-ALL by day 17 (disease #2; Figure 2D) and day 19 (disease #11; data not shown) after transplantation. Strikingly, Doxy therapy (Doxyl<sup>ther</sup>) reverted symptomatic disease, leading to complete clearance of neoplastic cells from the PB and BM, normalization of severe anemia and thrombocytopenia and convalescence of the animals within 10 days (Figure 2D and Movie S1). Additional experiments confirmed that intravenous injection of as few as 25,000 neoplastic B-cells into healthy mice reproducibly gave rise to leukemia, which was lethal within 2-3 weeks (Figure 2E). Local and systemic disease was also propagated by subcutaneously

implanting neoplastic B-cells recovered from enlarged lymph nodes, although with a longer latency (data not shown). In all these experiments, Doxy therapy rescued the majority of mice transplanted with neoplastic B-cells carrying the tetracycline repressible miR-126 expressing vector (Figure 2E) by clearing the blasts from the circulation and the BM (Figure 2F and not shown) and leading to the regression of solid tumor masses within a week, by a mechanism involving the induction of apoptosis (Figures S4D-E). In stark contrast, mice transplanted with B-cell neoplasms induced by the constitutive SFFV-126/OE vector (i.e. not responsive to Doxy treatment) succumbed to their disease when under Doxy treatment (Figure 2E). These data prove that tumors arising in the context of forced miR-126 expression are exquisitely vulnerable to withdrawal of this miR.

### **Transcriptional profiling of miR-126-deprived leukemia unveils an oncogenic program orchestrated by miR-126**

To uncover the molecular mechanisms underlying miR-126 addiction in leukemia we measured transcriptional changes occurring in a Tet.126 murine leukemia (#8) early after Doxy-mediated miR-126 shut-down. We performed RNA sequencing (RNAseq) of leukemic blasts purified from mouse BM at baseline and at 24, 48 and 72 hr after *in vivo* Doxy administration (Figure 3A). As expected, Doxy induced a time-dependent reduction in OFP and miR-126 expression (Figure 3B) confirming a near-complete silencing of the Tet.126 vector cassette by 72 hr. We identified 4,754 genes with a significant overtime variation following Doxy (Figure S5), 1,518 of which were progressively up-regulated over 72 hr of Doxy and pointed to the cell cycle, apoptosis, BCR signaling and cancer as the top regulated KEGG pathways (Figure 3C and Table S3). Clustering for biological processes overrepresented in the up-regulated gene dataset (GO analysis;  $p_{adj}<0.01$ , Z-score  $<-1.5$ ) further highlighted the centrality of cell cycle regulation and DNA replication (Figure S5C). In particular, we noted upregulation of negative cell cycle regulators and DNA repair components including Rb1, Cdkn1b, Cdkn2c, Chek1/Clspn, E2f7, Pml, several Rad proteins, the Bard1/Brca1 tumor suppressor complex and members of the Fanconi anemia complementation group (Figure 3D). We thus investigated cell cycle progression during miR-126 withdrawal in Tet.126 B-ALL by Ki67/Hoechst staining and

nucleoside incorporation following a 24 hr EdU pulse (Figure S6A-C). At 24 hr post Doxy, we noted an early recruitment into cell cycle followed, at 48 and 72 hr, by a significant increase of cells in G<sub>0</sub> and a decrease in late G<sub>1</sub> phase, compatible with cell cycle arrest. In addition, genes associated with leukocyte activation and B-cell functions were up-regulated in miR-126-depleted B-ALL blasts including key transcription factors driving B-cell development (Myb, Mafb, Ebfl, Ikzf1/3, Pbx1), genes involved in V(D)J recombination (Rag1/2, Lig4), (pre-)BCR signaling (Lyn, Syk, Fos), CD79a/b, CD127 (Il7ra) and CD20 (Figures 3C,E). Accordingly, miR-126 withdrawal seems to convert a Stat5-driven signaling environment to a pre-BCR-type signaling, as further suggested by downregulation of Jak3, Stat5a, Stat5b and upregulation of Bcl6 (Figure S6D). On the other hand, 1,606 DEGs were progressively down-regulated over 72 hr of Doxy. These genes comprised an exhaustive list of ribosomal proteins and GO categories related to RNA processing, translation and protein localization (not shown). Moreover, genes related to sugar metabolism were down-regulated. We postulate that some of these effects are due to Doxy treatment, as previously described (Moullan et al., 2015). Notably, most of the genes mapping to these latter pathways are excluded when applying a fold change cutoff of >2. With this more stringent cutoff, GO analysis (Figure S5D) and KEGG/Reactome pathway clustering (Figure 3F and Table S3) pointed to cell migration, coagulation and signal transduction, with a particular highlight on c-Kit signaling, as the principal pathways enriched in the down-regulated gene list. Interestingly, several oncogenes with a known role in leukemia/lymphoma were contained in this list including Ccnd1, Bcl2, Kit, Src, Eif4ebp1, Vav3, Lck and Tert, as well as several components of the Wnt signaling pathway (Figures 3F-G and S6D). Taken together, these data suggest that turning miR-126 off in our spontaneous leukemia model leads to the down-regulation of oncogenic/pro-survival signaling pathways and up-regulation of cell cycle, DNA damage response genes (including tumor suppressors) and genes associated with successive steps of B-cell differentiation and function.

### **Aberrant miR-126 expression downregulates p53 activity in hematopoietic progenitor cells**

The function of miR-126 in HSC is conserved between mice and humans (Lechman et al., 2012). In order to detect a potential effect of miR-126 on human progenitor cells, we transduced cord blood (CB) CD34<sup>+</sup> HSPC with a miR-126/OE, miR-126 knock-down (126/KD) or control LV. As expected, 126/OE decreased, while 126/KD increased short-term engraftment in NSG mice (Figure 4A). Interestingly, we noted a relative increase in circulating CD19<sup>+</sup> B lymphocytes in the transduced miR-126/OE graft (Figure 4B), and these cells were biased towards a CD10<sup>+</sup>CD20<sup>-</sup> immunophenotype (Figure 4C), strongly reminiscent of the maturation block and B-cell precursor spike observed in murine miR-126/OE hematopoiesis early after transplantation. RNAseq on sorted CD133<sup>+</sup>CD38<sup>-</sup> (referred to as CD38<sup>-</sup>) HSPC and CD133<sup>+</sup>CD38<sup>+</sup> (referred to as CD38<sup>+</sup>) progenitor cells after 126/KD or 126/OE yielded 79 and 32 high confidence transcripts that behaved as miR-126 targets (up in KD, down in OE) and anti-targets (down in KD, up in OE), respectively (Figures 4D-E and S7). Gene ontology analysis unveiled apoptosis, cell cycle regulation and p53 signaling as the most significantly enriched categories (Figure 4F). Pathway enrichment analysis using the KEGG, Wiki, Reactome and Biocarta databases (Table S4) or pre-ranked Gene Set Enrichment Analysis (Figure 4G) produced similar results again pointing to p53, cell cycle, apoptosis, PI3K/AKT signaling, cytokine-cytokine receptor interaction and cancer-associated pathways as significantly regulated by miR-126. This prompted us to analyze p53 protein localization by immunofluorescence staining in human CD34<sup>+</sup> CB HSPC and mouse Lin<sup>-</sup> HSPC transduced with 126/OE- or Ctrl LVs. The p53 staining pattern was strikingly different between the two treatment groups: while most Ctrl-transduced or untransduced HSPC showed a nuclear p53 staining pattern, >50% of 126/OE HSPC showed cytoplasmic p53 staining, which partially overlapped with proteasomal structures (Figure 5A-C). These data suggest that 126/OE increases nuclear export and proteasomal degradation of p53. To gain further independent evidence for this contention we exploited a p53 reporter plasmid, which allows measuring p53 transcriptional activity. We nucleofected the p53 reporter into CD34<sup>+</sup> CB-cells or murine Lin<sup>-</sup>Kit<sup>+</sup>Sca-1<sup>+</sup> cells and confirmed a significant reduction of p53 transcriptional activity upon 126/OE (Figure 5D), providing functional proof that the p53 pathway is negatively regulated by miR-126 in HSPC. Notably, effects on p53 were also seen at lower doses of miR-126 overexpression (driven from a vector containing the weaker EF1a promoter) and with a vector containing a seed mutation

in miR-126-5p (Figure 5E). In sharp contrast, mutating the seed of miR-126-3p abrogated the phenotype, suggesting that the 3p-strand of miR-126 is mainly responsible for downregulating p53 activity.

### **Dominant negative p53 mutant alleviates miR-126 addiction in the B-ALL mouse model**

To identify functionally relevant pathways mediating miR-126 addiction in our Tetracycline-repressible B-ALL mouse model, we performed rescue experiments with a dominant negative p53 (GSE56) or Ikaros (IK6) mutant (Milyavsky et al., 2010; Theocharides et al., 2015) probing the senescence/apoptosis and B-cell differentiation pathways, respectively. Tet.126 blasts (ALL#11) were lentivirally transduced with a GSE56/GFP-, IK6/NGFR- or Control/GFP-vector and transplanted into sublethally irradiated recipient mice. After 10 days all mice showed similarly high GFP<sup>+</sup> or NGFR<sup>+</sup> circulating blast counts indicating lack of effect of the dominant negative GSE56 and IK6 on disease engraftment and growth (Figure 6A). We then started Doxy treatment to turn off miR-126, and after 48 hr (d12) we noted significantly higher blast counts in the GSE56 group respect to Control or IK6. Interestingly, in some mice combination of GSE56 and IK6 further reduced the response of Tet.126 ALL to Doxy, with one mouse dying at 24 hr and 2 mice showing substantially higher blast counts at 48 hr than any other group (Figure 6A). Yet, all mice surviving beyond 24 hr eventually cleared the disease. We observed a similar effect of GSE56 expression in a Tet.126 ALL subclone that had become less responsive to Doxy with respect to the original disease (ALL#8). GSE56 conferred a significant advantage to the blasts leading to shortened survival of the mice (Figure 6B). Taken together, these data indicate that expression of a dominant negative p53 can partially rescue miR-126 addiction in B-ALL and point to a functionally relevant but not exclusive role of the p53 pathway downstream miR-126 in established B-ALL.

### **miR-126 targets genes related to p53 signaling**

To identify putative direct miR-126 targets responsible for these phenotypes, we interrogated 5 established target prediction algorithms ("miRWalk" platform) creating candidate lists of murine and human miR-126 targets that were independently

predicted by at least 2 algorithms. We then intersected the predicted targets with up-regulated genes (72 hr Doxy vs. basal) in the mouse leukemia RNAseq dataset or genes showing target-like behavior in one of the huCB RNAseq lists (Figure 6C and Table S5). Several previously published miR-126 targets were among the top candidates, including PIK3R2, PLK2, SPRED1 and VCAM1. We then focused on validating miR-126 targets that were linked with the p53 signaling pathway. In particular, cyclin dependent kinase inhibitor 2a interacting protein (Cdkn2aip), a positive regulator of p53 activity (Hasan et al., 2009), was a top candidate. Dual-luciferase assay confirmed direct regulation of the Cdkn2aip 3'UTR by miR-126 (Figure 6D). Moreover, Cdkn2aip mRNA expression was significantly lower in BM cells from 126/OE mice as compared to controls (not shown), and expression levels inversely correlated with those of miR-126 suggesting that Cdkn2aip expression is down-regulated by miR-126 *in vivo* in pre-leukemic miR-126/OE hematopoiesis. Additional candidate targets were tested using a bidirectional lentiviral (Bd.LV) reporter vector-based assay (Figure 6E,F), which validated Cdkn2aip, Axl, TNFRSF10B, PARP1, TRIM8, EDA2R and, possibly, KAT2B as direct miR-126-3p/5p targets.

### **Functional relevance of miR-126 expression in primary human B-ALL**

To investigate whether miR-126 expression could have a functional role in established human leukemia, we measured miR-126 levels in diagnostic BM aspirates from adult patients with ALL (n=17) (Figure 7A). Sixteen out of 17 ALL samples expressed miR-126 to levels higher than PBMCs or normal BM B-cells, and some of them reached the range observed in normal CD34<sup>+</sup> CB cells or in the matched CD34<sup>+</sup> BM cells collected upon achievement of complete remission (Figure 7B). Of note, miR-126 levels did not correlate with the expression of its host gene, *EGFL7* (Figure S8A), suggesting initiation at an internal CpG island with promoter activity (Li et al., 2008). Interestingly, individual diseases from our experimental murine B-ALL model also showed variable degrees of miR-126 overexpression, suggesting that the extent of miR-126 expression could be a disease-specific feature in B-ALL (Figure S8B).

Finally, we wanted to assess whether perturbing miR-126 expression had any functional impact on ALL blasts. We chose 5 representative Philadelphia chromosome (Ph)<sup>+</sup> ALL cases (11-177, 10-468, 12-150, 10-457 and 11-4966) with a

spectrum of miR-126 expression levels ranging from low to high. We optimized transduction conditions reaching up to 85% gene transfer and, in case of the 126/KD vector, de-repression of the OFP marker in a good fraction of cells (Figures 7C and S8C), an indication of successful inhibition of miR activity (Gentner et al., 2009). Transduced ALL blasts from the 5 representative patients were transplanted at non-limiting doses ( $>10^6$  blasts/mouse) into sublethally irradiated NSG mice. All mice engrafted ( $> 1\%$  human CD45 $^+$  cells in the PB) by 8-12 weeks and were subsequently euthanized for BM analysis. In 3 out of 5 diseases, we recovered a sufficient number of cells to allow sorting of transduced blasts and secondary transplantation into non-irradiated recipient NSG mice. In 4 out of 5 diseases, 126/KD resulted in a significantly reduced primary (1BM) and/or secondary (2BM) graft as compared to Ctrl-transduced cells (Figure 7D). In case of 11-4966, the disease with highest miR-126 expression, the phenotype was less pronounced in the BM of the secondary transplanted mice (2BM), possibly due to *in vivo* selection of 126/KD LV-transduced cells with incomplete miR-126 inhibition. However, serial PB samplings of the secondary transplanted mice demonstrated a significant delay in leukemia onset for the 126/KD group (Figure 7E). Instead, 126/KD did not have an appreciable impact on engraftment potential in 1 out of 5 diseases (12-150), a disease which ranged in the lower end of miR-126 expression (Figure 7A). Regarding the mechanism of reduced human B-ALL engraftment upon 126/KD, we measured proliferation rate and apoptosis levels in the transduced blasts. 126/KD did not change cell cycle distribution in B-ALL blasts as determined by Ki67/Hoechst staining and *in vivo* EdU incorporation studies (Figure S8D-E). However, we noted increased levels of apoptosis *in vitro* (Figure S8F) and *in vivo* (Figure 7F) following 126/KD as compared to control LV-transduced cells.

Taken together, these data indicate that reducing miR-126 activity negatively affects engraftment in the majority of tested Ph $^+$  B-ALL cases by increasing apoptosis levels, similar to the mouse leukemia model where blasts undergo widespread apoptosis after miR-126 withdrawal. These data indicate that aberrant expression of miR-126 is functionally important in a clinically relevant context and might represent a therapeutic target for ALL.

## DISCUSSION

Acute lymphoblastic leukemia most frequently originates from B-cell precursors that have acquired alterations in genes regulating lymphoid development, the cell cycle, the p53-retinoblastoma tumor suppressor pathway, cytokine receptor signaling and the epigenetic state (Hunger and Mullighan, 2015). We here show that forced expression of miR-126 in HSC and their progeny recapitulates many of these cardinal features by inducing B-ALL, and is required to maintain blast proliferation without inducing apoptosis or differentiation. Tumor addiction to a single oncogene has been described for miR-21 (Medina et al., 2010), miR-125a (Guo et al., 2012), miR-155 (Cheng et al., 2015) and few other oncoproteins including BCR-ABL1, c-Myc, Ras and Braf. Our work adds to the evidence that single miRs can orchestrate complex oncogenic programs, on a par with well-established protein coding oncogenes.

Sustained miR-126 expression has direct effects on the B-cell precursor compartment, including early lymphoid lineage priming (Okuyama et al., 2013), increased proliferation (Lechman et al., 2012) and - as shown in this work - reduced levels of apoptosis and delayed differentiation towards mature B-cells. It is likely that collaborating mutations occur at the level of multipotent progenitors and/or B-cell precursors in order to induce full-blown leukemia, and additional studies are warranted to define their nature and hierarchical occurrence in distinct progenitor cell subpopulations during the preleukemic phase in our model.

Our current work highlights differences in the response of HSC and lymphoid progenitors to miR-126/OE. Whereas HSC become excessively quiescent due to attenuated PI3K/AKT/GSK3 $\beta$  signaling (Lechman et al., 2012), this axis cannot explain the B-cell precursor phenotypes or miR-126 addiction in B-ALL. RNAseq analyses on human CB CD34 $^{+}$  progenitor cell subsets and murine B-ALL following modulation of miR-126 activity pointed to cell cycle regulation, apoptosis and p53 signaling as previously unrecognized miR-126 target pathways. Together with p16 $^{\text{Ink4a}}$  and p19 $^{\text{Arf}}$ , p53 has a central role in limiting the expansion potential of multipotent progenitors (Akala et al., 2008). Functional p53 inactivation by miR-126 might overcome this physiologic proliferation block and promote the accumulation of apoptosis-deficient B-cell precursors prone to transformation by mutations generated during aberrant V(D)J recombination, as seen in multiple p53-deficient mouse models (Donehower et al., 1992; MacPherson et al., 2004; Olive et al., 2004).

In established B-ALL, miR-126 withdrawal induced a dramatic disease regression paralleled by upregulation of a plethora of cell cycle regulators, and in particular genes associated with cell cycle arrest, apoptosis and DNA repair. A plausible interpretation for this result is that miR-126 inhibits a senescence response induced by oncogenes, chromosomal aberrations or inappropriate B-cell antigen receptor (BCR) signaling events inherent to the leukemia, which is triggered once miR-126 levels fall below a threshold. Transducing B-ALL with a dominant negative p53 mutant significantly delayed this response when turning miR-126 off, confirming that the p53 pathway is a central downstream effector of miR-126 also in established B-ALL. Conversely, restoration of p53 activity has been shown to induce tumor regression in several leukemia models (Velasco-Hernández et al., 2013; Ablain et al., 2014). In the mouse, we show that the stress response gene Cdkn2aip is one of the miR-126 targets likely contributing to the phenotype (Hasan et al., 2009). Also Plk2, a previously validated miR-126 target (Li et al., 2008) and a p53 target gene regulating the cell cycle and DNA damage response, which is frequently silenced in B-cell and myeloid malignancies, is likely to be relevant (Syed et al., 2006). Moreover, we here validate a number of additional miR-126 targets that act up- or downstream of p53, including TNFRSF10B and PARP family proteins, in line with a model of cooperative, multi-level p53 regulation by miR-126.

B-ALL generally contains 10-20 non silent coding mutations concomitantly altering multiple cellular growth, signaling and tumor suppression pathways (Hunger and Mullighan, 2015). It is therefore not surprising that a dominant negative p53 alone cannot fully rescue the disease once miR-126 has been shut off, whereas it strengthens the hypothesis that miR-126 orchestrates an oncogenic program in our B-ALL model where p53 inhibition is one important but not exclusive function of miR-126. Our RNAseq analysis on Tet.126 B-ALL provides further insights into this oncogenic program of miR-126. Notably, several stem cell- and cancer-associated pathways/genes show high basal expression and are down-regulated when miR-126 is turned off, most notably Kit signaling, Wnt signaling, Cyclin D1, Bcl2 and Thy1 (Figures 3G and Table S3). Mechanistically, enhanced signaling could occur through regulation of a signal transduction inhibitor by miR-126. One such candidate is represented by the ERK inhibitor Spred1, which is directly targeted by miR-126 (Wang et al., 2008), is up-regulated upon miR-126 silencing in our leukemia and is emerging as a tumor suppressor in ALL and AML (Olsson et al., 2014). Moreover,

Spred1 has recently been proposed as a key target responsible for the oncogenic activity of miR-126 when combined with AML-ETO1 (Li et al., 2015). On the other hand, it appears that many genes associated with B-cell differentiation are suppressed in 126/OE mouse leukemia cells, leading to a shift from Stat5 to pre-BCR signaling when turning miR-126 off. STAT5 activation is a hallmark of oncogenic cytokine receptor signaling in B-ALL (Muschens. 2015), and pre-BCR activation can trigger negative selection checkpoints in B-ALL resulting in cell death (Chen et al., 2015). In conclusion, these data suggest that miR-126 maintains B-ALL in a more primitive developmental state and prevents pre-BCR signaling. A similar role is carried out by Ikaros (IKZF1) loss-of-function mutants frequently found in high-risk ALL (Churchman et al., 2015). Emerging data suggest that these *Ikzf1* mutants alter adhesion of B-ALL blasts to stromal niches thereby profoundly influencing their proliferation, survival and sensitivity to tyrosine kinase inhibitors (Churchman et al., 2015; Joshi et al., 2015). Key adhesion molecules such as Thy1, Itga5 and Itgb1 and GO categories associated with the cytoskeleton and migration were down-regulated upon Doxy administration to Tet.126 ALL warranting further investigation of a potential link between miR-126 and cell motility. Interestingly, the dominant negative IK6 mutant acted synergistically with dominant negative p53 in rescuing blasts from miR-126 withdrawal in some mice. These data need to be confirmed in future studies systematically exploring combined genetic modifications to deconvolute the complex oncogenic activities of miR-126 in B-ALL, yet they indicate that the p53 and B-cell differentiation pathways are both functionally relevant for our miR-126 phenotype.

Our model has implications for human disease. Since a naturally-occurring miR-126 gain-of-function event in HSC would likely be counter-selected due to induction of an excessively quiescent state (Lechman et al., 2012), it is likely that aberrant miR-126 expression is installed at the progenitor level, probably by epigenetic mechanisms as seen in CBF leukemia (Li et al., 2008). The adult human B-ALL examined in this study expressed miR-126 at levels that ranged from low to high. This is in line with published miR profiling studies that found miR-126 expression in a variety of ALL subtypes including those with TEL-AML1 and BCR-ABL1 (Ph) translocations (Fulci et al., 2009; Schotte et al., 2011; Akbari-Moqadam et al., 2014). Interestingly, higher miR-126 expression has been correlated with chemotherapy resistance and poorer outcome (Schotte et al., 2011). Our mouse model offers a potential explanation for this observation, by linking miR-126 to p53 down-

regulation and IKAROS loss-of-function phenotypes. Mutations leading to loss of p53 and IKAROS function represent two principal clinical risk factors in B-ALL (Hof et al., 2011; Hunger and Mullighan, 2015). This association is further corroborated by our functional miR-126 knockdown studies on primary human Ph<sup>+</sup>ALL cells, where we noted –across a wide range of baseline miR-126 expression levels- induction of apoptosis and reduced engraftment in a xenotransplant model. We propose that miR-126 constitutes part of the armamentarium of human B-ALL cells to counteract apoptosis and differentiation thereby permanently maintaining them in an otherwise unstable progenitor cell state.

In AML, miR-126 is enriched in leukemic stem cells (LSC) where it regulates cell cycle, thereby maintaining the LSC pool and conferring resistance to chemotherapy (Lechman et al, 2016). While ALL is generally regarded as a disease composed of different subclones, which cannot be described by a classical stem cell model, a common theme between ALL and AML is their vulnerability to reductions in miR-126 levels (De Leeuw et al., 2014; Lechman et al, 2016). The obligate dependence of acute leukemia - in stark contrast to normal HSC- on adequate levels of miR-126 expression opens up a therapeutic window that can be exploited in patients with hematologic malignancies. The rationale for developing therapeutic strategies that target miR-126 in leukemia patients is two-fold: (1) Reducing miR-126 expression in normal HSC can expand their numbers without causing exhaustion or malignant transformation, thus boosting hematologic recovery; (2) Antagonizing miR-126 in leukemia counteracts chemotherapy resistance, impairs leukemia propagating cells and induces apoptosis. Developing pharmacologic agents that target miR-126 and/or its pathways may thus have the potential to improve the outcome of patients with acute leukemia.

## EXPERIMENTAL PROCEDURES

### Mouse Strains

B6.SJL-Ptprca, C57BL/6NTac-Ptprcb (both from Charles River) and NOD.Cg-Prkdc<sup>scid</sup>Il2rg<sup>tm1Wjl</sup>/SzJ (NSG) mice (The Jackson Lab) were maintained in specific-pathogen-free conditions following approval by our Institutional Animal Care and Use Committee (IACUC #455, #600, #618) and communication to the authorities as required by Italian law. Transplantation procedures are outlined in Supplementary Methods.

### Human Samples

CD34<sup>+</sup>CB-cells were purchased from Lonza. Primary ALL patient samples were obtained from the San Raffaele Hematologic Malignancies Biobank. All patients have provided informed consent to participate in the protocol. The research proposal has been reviewed and approved by an institutional review board and meets all requirements of the Declaration of Helsinki. Samples were centrally processed within 24 hr of their withdrawal during BM aspiration performed for diagnostic purposes.

### Modulation of microRNA activity

Lentiviral vector platforms for ectopic miRNA expression and stable knockdown were described previously (Lechman et al., 2012). High titer, concentrated LV stocks were used to stably transduce murine Lin-cells, CB CD34<sup>+</sup> cells and primary human ALL blasts, as described in Supplementary Methods.

### Flow Cytometry, confocal imaging, histopathology, standard molecular biology

A detailed description of experimental procedures can be found in Supplementary Methods.

### RNA sequencing

Sample libraries were prepared by the Ovation RNA-Seq system V2 (Nugen) and read on a HiSeq 2500 using the TruSeq PE protocol (Illumina). Technical details and bioinformatics analyses are described in Supplementary Methods.

## **General Statistical Analysis**

Unless otherwise indicated, mean  $\pm$ SEM values are reported in the graphs. For pairwise comparisons, a Student's t test (paired if appropriate) was used unless otherwise indicated. For three or more matched groups, a one-way analysis of variance (ANOVA) for repeated measures using a Bonferroni post-test correction was used. Percentages were transformed into a log-odds scale ( $\log(n\%(100-n\%))$ ).

## **ACCESSION NUMBERS**

RNA sequencing data have been submitted to Gene Expression Omnibus (<http://www.ncbi.nlm.nih.gov/geo>), and the following accession number has been assigned: GEO:GSE78078.

## **AUTHOR CONTRIBUTIONS**

S.N. and A.G. designed, performed and analyzed experiments and helped writing the paper. F.E.B. set up and performed RNA sequencing and bioinformatic data analysis. A.C. performed integration site and clonal tracking analysis. T.P., C.F., A.R., F.B. performed experiments. J.G.M. and D.C. performed and supervised RNA sequencing. E.R.L. and J.E.D. provided reagents and gave intellectual input. M.P. performed histopathologic analysis. F.C. provided patient samples and intellectual input. E.M. analyzed data and supervised experiments regarding integration site analysis. B.G. conceived the study, performed and supervised experiments, analyzed and interpreted the data, coordinated the research and wrote the paper. L.N. provided financial support, supervised and coordinated research and edited the paper.

## **ACKNOWLEDGEMENTS**

We thank D. Lazarevic, E. Stupka and M.Bianchi for RNAseq; L. Sergi Sergi, E. Tenderini, M. Rocchi A. Innocenzi, D. Biancolini for technical help; E. Zonari, P. Genovese, G. Schirolì, G. Spinozzi and G. Escobar for experimental help and fruitful discussions; C. Villa, S. Di Terlizzi, E. Canonico and M. Romano' for cell sorting; C. Covino for confocal imaging; C. Tresoldi, G. Nastasi and the Hematology and Bone

Marrow Transplant Unit for ALL samples. We thank S. Bertilaccio and G. Galletti for help with Ig rearrangement and S.E. Jacobsen and H. Doolittle for support to A.G. This work was supported by grants to L.N. from Telethon (TIGET grant), the EU (ERC Advanced Grant 249845 TARGETINGGENETHERAPY) and the Italian Ministry of Health, and by an EHA Clinical Research Fellowship to B.G.

## FIGURE LEGENDS

### Figure 1. Ectopic miR-126 expression in HSPC induces leukemia

(A) Mice were transplanted with either miR-126/OE- or control (Ctrl)-LV transduced HSPC. Leukemia incidence for the 126/OE- (blue) and control group (grey) is plotted below (representative experiment). Log-rank test (Mantel-Cox)  $p=0.0197$ . (B) Representative immunophenotyping of  $CD19^+$  PB cells at 4 weeks post transplant and quantification of  $OFP^+CD45^{\text{low}}$  cells (min to max Whiskers plots) within the  $CD19^+$  B-cell compartment. ( $n=12$  OE mice,  $n=9$  Ctrl mice; data represent means  $\pm$  SEM;  $p <0.0001$ , two-way ANOVA). (C) Expansion of  $CD45^{\text{low}}$  cells over time in a representative mouse, before evolution to frank ALL. (D) Complete blood counts (WBC: white blood cell counts; HGB: Hemoglobin; PLT: platelets) of mice at leukemia diagnosis compared to healthy controls. Red dotted lines represent normal reference values. (E) Representative peripheral blood smear of a mouse diagnosed with ALL (M&G staining). (F) Histopathology of indicated organs from mice diagnosed with ALL (H&E staining). (G) Representative B-ALL immunophenotype. (H) Sharing between tumor core IS (mice A0, B1, C1, C4, C3, A1) and normal PB lineages prospectively sampled from the corresponding mice during the pre-leukemic phase (25 to 153 days after transplantation). The color scale indicates the relative abundance of individual IS. PB subpopulations were sorted as follows: Myeloid:  $CD11b^+$ ; B-cells:  $CD19^+CD45^{\text{hi}}$ ; T cells:  $CD3^+$ ; Immature B-cells:  $CD19^+OFP^+CD45^{\text{low}}$  (sampled at least 31-68 days before occurrence of the first tumor). See also Figures S1, S2, S3 and Tables S1, S2.

### Figure 2. Leukemia is addicted to miR-126 expression

(A) Tet-off miR-126/OE system. Murine  $\text{Lin}^-$  cells were sequentially transduced with LVs (I) and (II), and transplanted into  $n=14$  lethally irradiated primary recipients. 4 weeks later, whole BM from each individual primary mouse was transplanted into 2 lethally irradiated secondary recipients, one of which preemptively received Doxycycline (Doxy<sup>PE</sup>) when  $CD19^+CD45^{\text{low}}$  cells appeared in the PB ( $n=11$ , 3 irradiation deaths), while the other was put on observation ( $n=14$  ‘no Doxy’). BM cells from mice that have developed malignancy were then transplanted into tertiary recipients assigned to prophylactic Doxy treatment (Doxy<sup>PROPH</sup>) or observation. Once diagnosed with leukemia, mice from the observation group were switched to Doxy

treatment with therapeutic intent (Doxy<sup>THER</sup>). (B) Representative FACS plots of CD19<sup>+</sup> PB cells in a matched no Doxy/Doxy<sup>PE</sup> secondary transplanted mouse pair 5d after Doxy. Quantification of CD45<sup>low</sup> B-cells in the PB of primary (1st) and secondary (2nd) transplant recipients at the indicated number of days post transplant and post Doxy<sup>PE</sup> administration (data represent means  $\pm$  SEM; \* p<0.05; \*\* p<0.01, paired t-test). (C) Leukemia incidence in the 'no Doxy' or Doxy<sup>PE</sup> group of secondary-transplanted mice. Log-rank test (Mantel-Cox) p=0.0247. (D) Leukemia engraftment and treatment response in representative, sublethally irradiated, tertiary transplanted mice. FACS plots show PB leukocyte populations at 14d post leukemia transplantation (Doxy<sup>PROPH</sup> and 'no Doxy') and follow-up of the 'no Doxy' mouse at 3 and 9d after Doxy<sup>THER</sup>. Note that almost all CD19<sup>+</sup> B-cells in the 'no Doxy' mouse were leukemic blasts (OFP<sup>+</sup>CD45<sup>low</sup>), while Doxy<sup>PROPH</sup> and Doxy<sup>THER</sup> eliminated CD45<sup>low</sup>OFP<sup>+</sup> cells. Graphs on the bottom show WBC, PLT counts and HGB levels in the Doxy<sup>PROPH</sup> (n=2) and no Doxy/Doxy<sup>THER</sup> (n=2) groups. Blue arrows indicate the start of Doxy<sup>THER</sup>. (E) Survival of mice injected with SFFV.126/OE leukemia (n=4 Doxy<sup>THER</sup>) or Tet.126/OE leukemia (n=7 Doxy<sup>THER</sup>, n=4 no Doxy). Survival was significantly better in the Tet.126/OE+Dox<sup>THER</sup> group respect to the other two groups (Log-Rank test p = 0.0002). (F) Kinetics of blast clearance (CD19<sup>+</sup>CD45<sup>low</sup> cells) from PB following Doxy<sup>THER</sup>. n=2 mice received IV grafts following sublethal irradiation; n=4 mice received IV grafts without irradiation; n=2 mice received subcutaneous ALL grafts. A total of 3 independent diseases were injected, Doxy response did not differ between different diseases or transplantation modalities. See also Figure S4 and Movie S1.

**Figure 3. Transcriptional changes in a miR-126-addicted leukemia following miR withdrawal**

(A) C57/BL6 mice were injected with an established Tet.126 leukemia, and BM blasts were purified from n=9 mice treated with PBS (Ctrl) and n=9 mice exposed to Doxy<sup>THER</sup> for 24, 48 or 72 hr (3 mice per timepoint) for RNAseq. (B) Doxy<sup>THER</sup> down-regulated vector-encoded OFP mean fluorescence intensity (MFI) and miR-126 expression in a time-dependent manner (n=3 representative samples per timepoint). (C) Bipartite graph shows significantly enriched KEGG pathways (P-adj<0.1) and their associated genes within the 1518 progressively up-regulated transcripts under Doxy<sup>THER</sup> in the RNAseq analysis. (D) Heatmap showing expression of cell cycle

regulators (first GO cluster in Figure S5C) in ALL blasts at baseline and following miR-126 downregulation (24, 48, 72 hr of Doxy exposure). (E) Heatmap showing expression of up-regulated genes mapping to the KEGG pathway "BCR signaling" and the GO:0045321 category "leukocyte activation". Cd38, Cd55, Il3 and Ciita were manually added. (F) RNAseq identified 340 genes that were progressively down-regulated in the Doxy-treated group with respect to control (fold change  $>2$  at 72 hr vs. baseline), and the bipartite graph shows selected top KEGG and Reactome pathway enrichments and their associated genes ( $p.\text{adj}<0.1$ ). (G) Heatmap showing expression of selected oncogenes in ALL blasts at baseline and following miR-126 downregulation (24, 48, 72 hr of Doxy exposure). See also Figures S5, S6 and Table S3.

**Figure 4. Ectopic miR-126 expression in human CB favors accumulation of B-cell precursors and downregulates p53-related transcripts**

(A) BM engraftment of human CB CD34 $^{+}$  cells transduced with Ctrl LV, 126/OE LV or 126/KD LV in NSG mice at the indicated timepoints (3 weeks: n=3 Ctrl, n=4 126/OE, n=4 126/KD mice; 4 weeks: n=3 Ctrl, n=7 126/OE, n=7 126/KD).  $p<0.001$  by two-way ANOVA, asterisks denote significant differences in the Bonferroni post-test. (B) B-cell contribution and (C) composition after short-term repopulation (3-4 weeks). Data are from 3 (B) and 2 (C) independent experiments, shown are the mean  $\pm$  SEM. Statistics by one-way ANOVA on transduced CD19 $^{+}$  (B) or CD19 $^{+}$ CD10 $^{+}$ CD20 $^{-}$  cells (C) with Bonferroni post-test correction. Significance levels: \*\*\*\*  $p <0.0001$ , \*\*\*  $p<0.001$ , \*\*  $p<0.01$ , \*  $p<0.05$ . (D) RNAseq on CB CD34 $^{+}$  subpopulations at 72 hr following transduction with 126/OE, 126/KD or Ctrl LVs. (E) shows the total number of differentially expressed genes (DEGs,  $p.\text{adj}<0.1$ ) for each group (black) and the number of DEGs broken down into up-regulated (red) and down-regulated genes (blue). (F) Gene ontology (GO) analysis of 79 DEGs showing miR target-like behavior (up upon 126/KD and/or down upon 126/OE) and 32 DEGs behaving inversely (top 5 GO categories with  $p.\text{adj}<0.05$ ). Only DEGs identified in at least 2 independent data lists were included. (G) GSEA enrichment plots for the highest scoring KEGG pathways obtained from gene lists pre-ranked according to log2FC in 126/OE and 126/KD vs. control, respectively, regardless of CD38 status. See also Figure S7 and Table S4.

**Figure 5. Ectopic miR-126 expression results in cytoplasmic p53 translocation and reduced transcriptional activity**

Human CB CD34<sup>+</sup> (A) or murine Lin<sup>-</sup> cells (B) were transduced with 126/OE or Ctrl LVs and analyzed for p53 protein expression on day 4 of culture. Shown are representative confocal immunofluorescence (IF) images and respective quantifications performed manually (fraction of cells with a clustered cytoplasmatic p53 staining pattern on 15 random high power fields; 4-78 cells per field) or semi-automatically (area overlap between p53 and nuclear staining). (C) Representative co-stainings of p53 and proteasomal components in CB CD34<sup>+</sup> cells. (D) Ctrl LV- or 126/OE LV-transduced CD34<sup>+</sup> CB-cells (n=3 donors, *left graph*) or murine Lin<sup>-</sup> Kit<sup>+Sca-1<sup>-</sup></sup> cells (n=2, *right graph*) were nucleofected with a p53 reporter plasmid, and Firefly (p53-responsive) to Renilla (transfection control) Luciferase activity was measured after 4-6 hr. Data represent means  $\pm$  SEM. (E) Fraction of nuclear p53 protein in CB CD34<sup>+</sup> cells measured by IF as in (A) after transduction with a panel of 126/OE LVs carrying seed mutants in miR-126-3p (SFFV.126SM) or -5p (SFFV.126\*SM) or a weaker promoter (EF1a.126). Data represent means  $\pm$  SEM p<0.0001, one-way ANOVA. Post-tests against ctrl: \*\*\*\*: p <0.0001, \*\*\* p<0.001\*\*\*, ns=not significant.

**Figure 6. Validation of miR-126 targets related to p53 signaling**

(A) Tet.126 ALL (#11) was transduced with one of the indicated LVs or a combination of GSE56- and IK6-LV expressing dominant negative p53 or IKZF1, respectively, and transplanted into sublethally irradiated recipients (n=6 per group). Transduction efficiency measured on OFP<sup>+</sup> blasts *in vivo* was 20-30% for all groups. Mice were put on Doxy from day 10. Graphs show an absolute quantification of GFP<sup>+</sup> and/or NGFR<sup>+</sup> ALL blasts in the PB at the indicated timepoints. One mouse from the GSE56/IK6 combi group died between day 10 and 11. Statistics were performed by one-way ANOVA considering only the single LV groups. \* p<0.05, \*\* p<0.01 in Bonferroni post-test. (B) Similar setup as in (A). A partially resistant Tet.126 ALL subclone (#8') was transduced either with a Ctrl LV or with GSE56 LV and injected into syngeneic, sublethally conditioned recipients (n=10 and 5, respectively). Disease engraftment and mice survival is shown. (C) Top target predictions for miR-126-3p crossing the miRWALK database with up-regulated transcripts in the mouse Tet.126

ALL #8 after miR-126 withdrawal (upper table) and transcripts with 'target-like' behavior in huCB CD34<sup>+</sup> cells (lower table). The table shows the number of algorithms that independently predict the candidate gene as a direct miR-126-3p or -5p target (maximum: 5 algorithms). (D) The scheme shows the proposed model of p53 regulation by Cdkn2aip according to published data. Luciferase assay confirms regulation of the murine Cdkn2aip 3'UTR by miR-126. Shown is the Renilla (transfection control)/Firefly (3'UTR responsive) LUC ratio in 126/OE 293T cells normalized to CTRL LV-transduced cells (n=12-15). Data represent means  $\pm$  SEM. The bottom graph shows an inverse correlation between miR-126 expression ( $2^{-\Delta^{CT}}$  versus miR-16) and Cdkn2aip transcript levels ( $2^{-\Delta\Delta^{CT}}$  versus HPRT) in individual mice from the 126/OE LV group.  $R^2=0.9848$ . (E) Validation of candidate miR-126-3p or (F) miR-126-5p (126\*) targets emerging from our RNAseq datasets by bidirectional reporter LV (BdLV) assay. Fold repression is calculated as follows: GFP MFI/Cherry MFI ratio (control BdLV) divided by GFP MFI/Cherry ratio (GFP.3'UTR containing BdLV). Data represent means  $\pm$  SEM \* p<0.05; \*\* p<0.01; \*\*\* p<0.001; n=3-10. See also Table S5.

**Figure 7. Antagonizing miR-126 in human B-ALL reduces disease burden in xenograft models**

(A) Expression of miR-126 in Ph<sup>+</sup> (BCR-ABL1<sup>+</sup>) or Ph<sup>-</sup> (other subtypes) B-ALL patient samples (median blast content: 85%, range: 59-93%) or PBMC/CD34<sup>+</sup> CB cells from healthy donors. Expression levels were normalized to U16 SNRRNA ( $2^{-\Delta^{Ct}}$ ) and calibrated to PBMC (mean of 2 replicates). (B) miR-126 expression ( $2^{-\Delta^{Ct}}$  against U16 SNRRNA) in CD34<sup>+</sup>CD19<sup>+</sup> purified Ph<sup>+</sup> B-ALL blasts and patient-matched normal B-cells (CD19<sup>+</sup>) or HSPC (CD34<sup>+</sup>) obtained from a corresponding post-remission sample. Refr.ALL: patient with refractory disease. Data from normal CD34<sup>+</sup> cells represent means of two serial sampling from the same patient. Mean  $\pm$  SEM is represented in the graph. (C) Ph<sup>+</sup> B-ALL primografts transduced with the 126/KD- or Ctrl-LV were generated, and transduced blasts were purified from the BM (FACS plots are representative) and transplanted into secondary recipients. (D) Engraftment of transduced (OFP<sup>+</sup>) B-ALL cells in the BM of primary recipients (1BM; 11-4966: n=5 Ctrl, n=2 126/KD, at 8 weeks; 10-457: n=5 Ctrl, n=6 126/KD, at 12 weeks; 10-468: n=3 Ctrl, n=3 126/KD, at 8 weeks; 11-177: n=5 Ctrl, n=4 126/KD,

at 8 weeks; 12-150: n=4 Ctrl, n=6 126/KD, at 12 weeks) or secondary recipients (2BM; 11-4966: n=7 Ctrl, n=3 126/KD, at 10 weeks; 10-457: n=3 Ctrl, n=3 126/KD, at 12 weeks; 12-150: n=5 Ctrl, n=5 126/KD, at 12 weeks). P values above the bars refer to unpaired t-tests; Statistical significance by two-way ANOVA is indicated next to the bracket in the graph legend (ns, not significant; \*: p<0.05, \*\*\*, p<0.001). Data represent means  $\pm$  SEM. (E) PB engraftment of secondary recipients transplanted with disease 11-4966. p= 0.026, two-way ANOVA. (F) Annexin V staining of 2BM from diseases 11-4966 and 10-457, statistics as in (D); data represent means  $\pm$  SEM. See also Figure S8.

## References

Ablain, J., Rice, K., Soilihi, H., de Reynies, A., Minucci, S., and de The, H. (2014). Activation of a promyelocytic leukemia-tumor protein 53 axis underlies acute promyelocytic leukemia cure. *Nat Med* 20, 167-174.

Akala, O. O., Park, I. K., Qian, D., Pihalja, M., Becker, M. W., and Clarke, M. F. (2008). Long-term haematopoietic reconstitution by Trp53-/p16Ink4a-/p19Arf-/multipotent progenitors. *Nature* 453, 228-232.

Akbari Moqadam, F., Lange-Turenhout, E. A., van der Veer, A., Marchante, J. R., Boer, J. M., Pieters, R., and den Boer, M. (2014). MicroRNA signature in BCR-ABL1-like and BCR-ABL1-positive childhood acute lymphoblastic leukemia: similarities and dissimilarities. *Leuk Lymphoma* 55, 1942-1945.

Amendola, M., Passerini, L., Pucci, F., Gentner, B., Bacchetta, R., and Naldini, L. (2009). Regulated and multiple miRNA and siRNA delivery into primary cells by a lentiviral platform. *Mol Ther* 17, 1039-1052.

Bartel, D. P. (2009). MicroRNAs: target recognition and regulatory functions. *Cell* 136, 215-233.

Blandino, G., Fazi, F., Donzelli, S., Kedmi, M., Sas-Chen, A., Muti, P., Strano, S., and Yarden, Y. (2014). Tumor suppressor microRNAs: a novel non-coding alliance against cancer. *FEBS Lett* 588, 2639-2652.

Bousquet, M., Harris, M. H., Zhou, B., and Lodish, H. F. (2010). MicroRNA miR-125b causes leukemia. *Proc Natl Acad Sci U S A* 107, 21558-21563.

Chen, Z., Shojaee, S., Buchner, M., Geng, H., Lee, J. W., Klemm, L., Titz, B., Graeber, T. G., Park, E., Tan, Y. X., *et al.* (2015). Signalling thresholds and negative B-cell selection in acute lymphoblastic leukaemia. *Nature* 521, 357-361.

Cheng, C. J., Bahal, R., Babar, I. A., Pincus, Z., Barrera, F., Liu, C., Svoronos, A., Braddock, D. T., Glazer, P. M., Engelman, D. M., *et al.* (2015). MicroRNA silencing for cancer therapy targeted to the tumour microenvironment. *Nature* 518, 107-110.

Chiriaco, M., Farinelli, G., Capo, V., Zonari, E., Scaramuzza, S., Di Matteo, G., Sergi, L. S., Migliavacca, M., Hernandez, R. J., Bombelli, F., *et al.* (2014). Dual-regulated lentiviral vector for gene therapy of X-linked chronic granulomatosis. *Mol Ther* 22, 1472-1483.

Churchman, M. L., Low, J., Qu, C., Paietta, E. M., Kasper, L. H., Chang, Y., Payne-Turner, D., Althoff, M. J., Song, G., Chen, S. C., *et al.* (2015). Efficacy of Retinoids in IKZF1-Mutated BCR-ABL1 Acute Lymphoblastic Leukemia. *Cancer Cell* 28, 343-356.

de Leeuw, D. C., Denkers, F., Olthof, M. C., Rutten, A. P., Pouwels, W., Schuurhuis, G. J., Ossenkoppele, G. J., and Smit, L. (2014). Attenuation of microRNA-126 expression that drives CD34+38- stem/progenitor cells in acute myeloid leukemia leads to tumor eradication. *Cancer Res* 74, 2094-2105.

Donehower, L. A., Harvey, M., Slagle, B. L., McArthur, M. J., Montgomery, C. A., Jr., Butel, J. S., and Bradley, A. (1992). Mice deficient for p53 are developmentally normal but susceptible to spontaneous tumours. *Nature* *356*, 215-221.

Eppert, K., Takenaka, K., Lechman, E. R., Waldron, L., Nilsson, B., van Galen, P., Metzeler, K. H., Poepl, A., Ling, V., Beyene, J., *et al.* (2011). Stem cell gene expression programs influence clinical outcome in human leukemia. *Nat Med* *17*, 1086-1093.

Fulci, V., Colombo, T., Chiaretti, S., Messina, M., Citarella, F., Tavolaro, S., Guarini, A., Foa, R., and Macino, G. (2009). Characterization of B- and T-lineage acute lymphoblastic leukemia by integrated analysis of MicroRNA and mRNA expression profiles. *Genes Chromosomes Cancer* *48*, 1069-1082.

Gentner, B., Schira, G., Giustacchini, A., Amendola, M., Brown, B. D., Ponzoni, M., and Naldini, L. (2009). Stable knockdown of microRNA in vivo by lentiviral vectors. *Nat Methods* *6*, 63-66.

Gentner, B., Visigalli, I., Hiramatsu, H., Lechman, E., Ungari, S., Giustacchini, A., Schira, G., Amendola, M., Quattrini, A., Martino, S., *et al.* (2010). Identification of hematopoietic stem cell-specific miRNAs enables gene therapy of globoid cell leukodystrophy. *Sci Transl Med* *2*, 58ra84.

Gruber, J. J., Zatechka, D. S., Sabin, L. R., Yong, J., Lum, J. J., Kong, M., Zong, W. X., Zhang, Z., Lau, C. K., Rawlings, J., *et al.* (2009). Ars2 links the nuclear cap-binding complex to RNA interference and cell proliferation. *Cell* *138*, 328-339.

Guo, S., Bai, H., Megyola, C. M., Halene, S., Krause, D. S., Scadden, D. T., and Lu, J. (2012). Complex oncogene dependence in microRNA-125a-induced myeloproliferative neoplasms. *Proc Natl Acad Sci U S A* *109*, 16636-16641.

Guo, S., Lu, J., Schlanger, R., Zhang, H., Wang, J. Y., Fox, M. C., Purton, L. E., Fleming, H. H., Cobb, B., Merkenschlager, M., *et al.* (2010). MicroRNA miR-125a controls hematopoietic stem cell number. *Proc Natl Acad Sci U S A* *107*, 14229-14234.

Han, Y. C., Park, C. Y., Bhagat, G., Zhang, J., Wang, Y., Fan, J. B., Liu, M., Zou, Y., Weissman, I. L., and Gu, H. (2010). microRNA-29a induces aberrant self-renewal capacity in hematopoietic progenitors, biased myeloid development, and acute myeloid leukemia. *J Exp Med* *207*, 475-489.

Hasan, K., Cheung, C., Kaul, Z., Shah, N., Sakaushi, S., Sugimoto, K., Oka, S., Kaul, S. C., and Wadhwa, R. (2009). CARF Is a vital dual regulator of cellular senescence and apoptosis. *J Biol Chem* *284*, 1664-1672.

He, L., Thomson, J. M., Hemann, M. T., Hernando-Monge, E., Mu, D., Goodson, S., Powers, S., Cordon-Cardo, C., Lowe, S. W., Hannon, G. J., and Hammond, S. M. (2005). A microRNA polycistron as a potential human oncogene. *Nature* *435*, 828-833.

Hof, J., Krentz, S., van Schewick, C., Korner, G., Shalapour, S., Rhein, P., Karawajew, L., Ludwig, W. D., Seeger, K., Henze, G., *et al.* (2011). Mutations and deletions of the TP53 gene predict nonresponse to treatment and poor outcome in first relapse of childhood acute lymphoblastic leukemia. *J Clin Oncol* 29, 3185-3193.

Hunger, S. P., and Mullighan, C. G. (2015). Acute Lymphoblastic Leukemia in Children. *N Engl J Med* 373, 1541-1552.

Joshi, I., Yoshida, T., Jena, N., Qi, X., Zhang, J., Van Etten, R. A., and Georgopoulos, K. (2014). Loss of Ikaros DNA-binding function confers integrin-dependent survival on pre-B-cells and progression to acute lymphoblastic leukemia. *Nat Immunol* 15, 294-304.

Lechman, E. R., Gentner, B., van Galen, P., Giustacchini, A., Saini, M., Boccalatte, F. E., Hiramatsu, H., Restuccia, U., Bachi, A., Voisin, V., *et al.* (2012). Attenuation of miR-126 activity expands HSC in vivo without exhaustion. *Cell Stem Cell* 11, 799-811.

Lechman E.R., Gentner B, Ng S.W., Schoof EM, van Galen P., Kennedy J.A., Nucera S., Ciceri F., *et al.* (2016). miR-126 Regulates Distinct Self-Renewal Outcomes in Normal and Malignant Hematopoietic Stem Cells. *Cancer Cell* 29(2):214-28.

Li, Z., Lu, J., Sun, M., Mi, S., Zhang, H., Luo, R. T., Chen, P., Wang, Y., Yan, M., Qian, Z., *et al.* (2008). Distinct microRNA expression profiles in acute myeloid leukemia with common translocations. *Proc Natl Acad Sci U S A* 105, 15535-15540.

Li, Z., Chen, P., Su, R., Li, Y., Hu, C., Wang, Y., Arnovitz, S., He, M., Gurbuxani, S., Zuo, Z., *et al.* (2015). Overexpression and knockout of miR-126 both promote leukemogenesis. *Blood* 126, 2005-2015.

MacPherson, D., Kim, J., Kim, T., Rhee, B. K., Van Oostrom, C. T., DiTullio, R. A., Venere, M., Halazonetis, T. D., Bronson, R., De Vries, A., *et al.* (2004). Defective apoptosis and B-cell lymphomas in mice with p53 point mutation at Ser 23. *EMBO J* 23, 3689-3699.

Medina, P. P., Nolde, M., and Slack, F. J. (2010). OncomiR addiction in an in vivo model of microRNA-21-induced pre-B-cell lymphoma. *Nature* 467, 86-90.

Milyavsky, M., Gan, O. I., Trottier, M., Komosa, M., Tabach, O., Notta, F., Lechman, E., Hermans, K. G., Eppert, K., Konovalova, Z., *et al.* (2010). A distinctive DNA damage response in human hematopoietic stem cells reveals an apoptosis-independent role for p53 in self-renewal. *Cell Stem Cell* 7, 186-197.

Moullan, N., Mouchiroud, L., Wang, X., Ryu, D., Williams, E. G., Mottis, A., Jovaisaite, V., Frochaux, M. V., Quiros, P. M., Deplancke, B., *et al.* (2015). Tetracyclines Disturb Mitochondrial Function across Eukaryotic Models: A Call for Caution in Biomedical Research. *Cell Rep*.

Muschen, M. (2015). Rationale for targeting the pre-B-cell receptor signaling

pathway in acute lymphoblastic leukemia. *Blood* *125*, 3688-3693.

O'Connell, R. M., Rao, D. S., Chaudhuri, A. A., Boldin, M. P., Taganov, K. D., Nicoll, J., Paquette, R. L., and Baltimore, D. (2008). Sustained expression of microRNA-155 in hematopoietic stem cells causes a myeloproliferative disorder. *J Exp Med* *205*, 585-594.

Okuyama, K., Ikawa, T., Gentner, B., Hozumi, K., Harnprasopwat, R., Lu, J., Yamashita, R., Ha, D., Toyoshima, T., Chanda, B., *et al.* (2013). MicroRNA-126-mediated control of cell fate in B-cell myeloid progenitors as a potential alternative to transcriptional factors. *Proc Natl Acad Sci U S A* *110*, 13410-13415.

Olive, K. P., Tuveson, D. A., Ruhe, Z. C., Yin, B., Willis, N. A., Bronson, R. T., Crowley, D., and Jacks, T. (2004). Mutant p53 gain of function in two mouse models of Li-Fraumeni syndrome. *Cell* *119*, 847-860.

Olsson, L., Castor, A., Behrendtz, M., Biloglav, A., Forestier, E., Paulsson, K., and Johansson, B. (2014). Deletions of IKZF1 and SPRED1 are associated with poor prognosis in a population-based series of pediatric B-cell precursor acute lymphoblastic leukemia diagnosed between 1992 and 2011. *Leukemia* *28*, 302-310.

Ooi, A. G., Sahoo, D., Adorno, M., Wang, Y., Weissman, I. L., and Park, C. Y. (2010). MicroRNA-125b expands hematopoietic stem cells and enriches for the lymphoid-balanced and lymphoid-biased subsets. *Proc Natl Acad Sci U S A* *107*, 21505-21510.

Schotte, D., De Menezes, R. X., Akbari Moqadam, F., Khankahdani, L. M., Lange-Turenhout, E., Chen, C., Pieters, R., and Den Boer, M. L. (2011). MicroRNA characterize genetic diversity and drug resistance in pediatric acute lymphoblastic leukemia. *Haematologica* *96*, 703-711.

Starczynowski, D. T., Kuchenbauer, F., Argiopoulos, B., Sung, S., Morin, R., Muranyi, A., Hirst, M., Hogge, D., Marra, M., Wells, R. A., *et al.* (2010). Identification of miR-145 and miR-146a as mediators of the 5q- syndrome phenotype. *Nat Med* *16*, 49-58.

Syed, N., Smith, P., Sullivan, A., Spender, L. C., Dyer, M., Karran, L., O'Nions, J., Allday, M., Hoffmann, I., Crawford, D., *et al.* (2006). Transcriptional silencing of Polo-like kinase 2 (SNK/PLK2) is a frequent event in B-cell malignancies. *Blood* *107*, 250-256.

Theocharides, A. P., Dobson, S. M., Laurenti, E., Notta, F., Voisin, V., Cheng, P. Y., Yuan, J. S., Guidos, C. J., Minden, M. D., Mullighan, C. G., *et al.* (2015). Dominant-negative Ikaros cooperates with BCR-ABL1 to induce human acute myeloid leukemia in xenografts. *Leukemia* *29*, 177-187.

Velasco-Hernandez, T., Vicente-Duenas, C., Sanchez-Garcia, I., and Martin-Zanca, D. (2013). p53 restoration kills primitive leukemia cells in vivo and increases survival of leukemic mice. *Cell Cycle* *12*, 122-132.

Wang, S., Aurora, A. B., Johnson, B. A., Qi, X., McAnally, J., Hill, J. A., Richardson, J. A., Bassel-Duby, R., and Olson, E. N. (2008). The endothelial-specific microRNA miR-126 governs vascular integrity and angiogenesis. *Dev Cell* 15, 261-271.

Xiao, C., Srinivasan, L., Calado, D. P., Patterson, H. C., Zhang, B., Wang, J., Henderson, J. M., Kutok, J. L., and Rajewsky, K. (2008). Lymphoproliferative disease and autoimmunity in mice with increased miR-17-92 expression in lymphocytes. *Nat Immunol* 9, 405-414.

# Figure 1

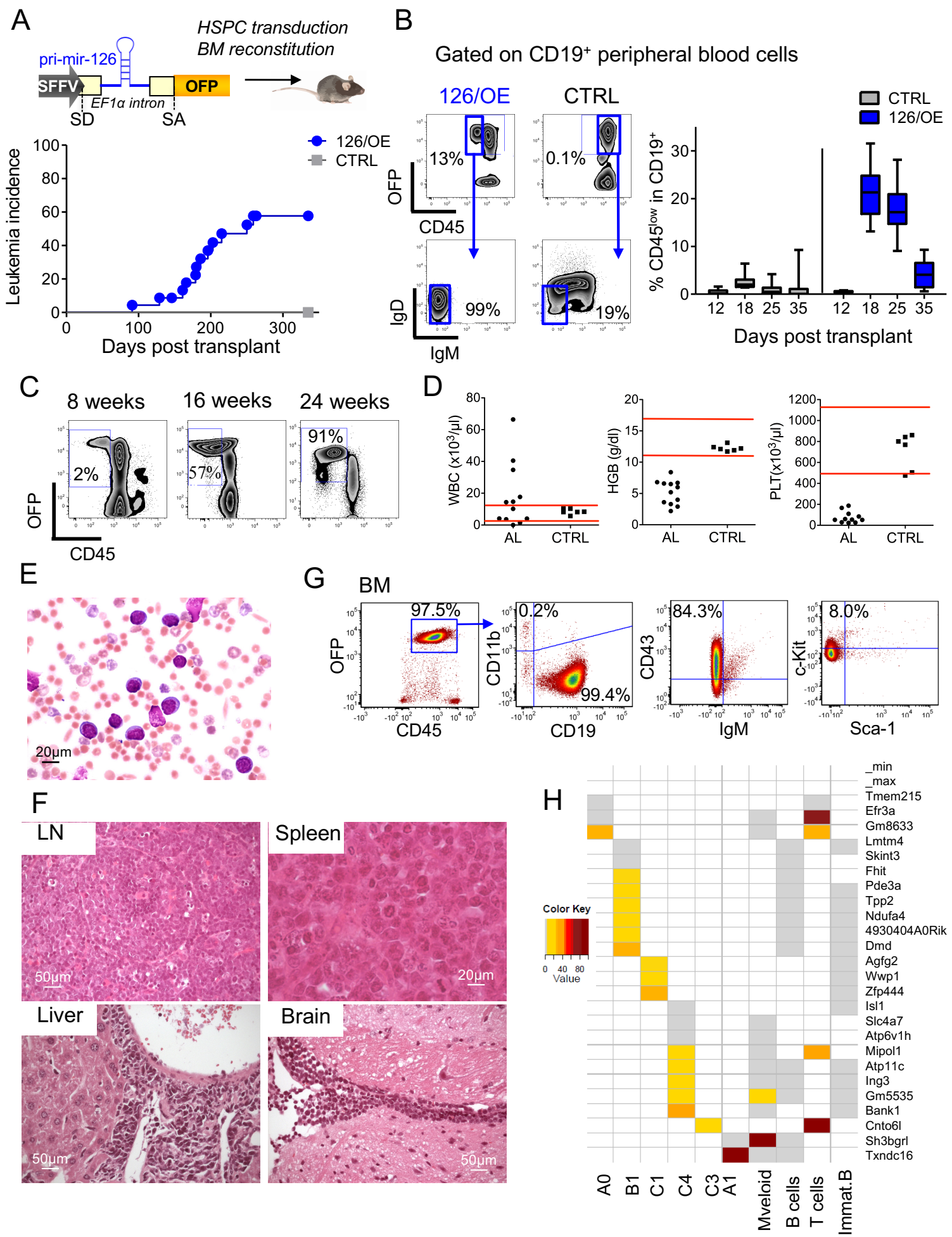


# Figure 2

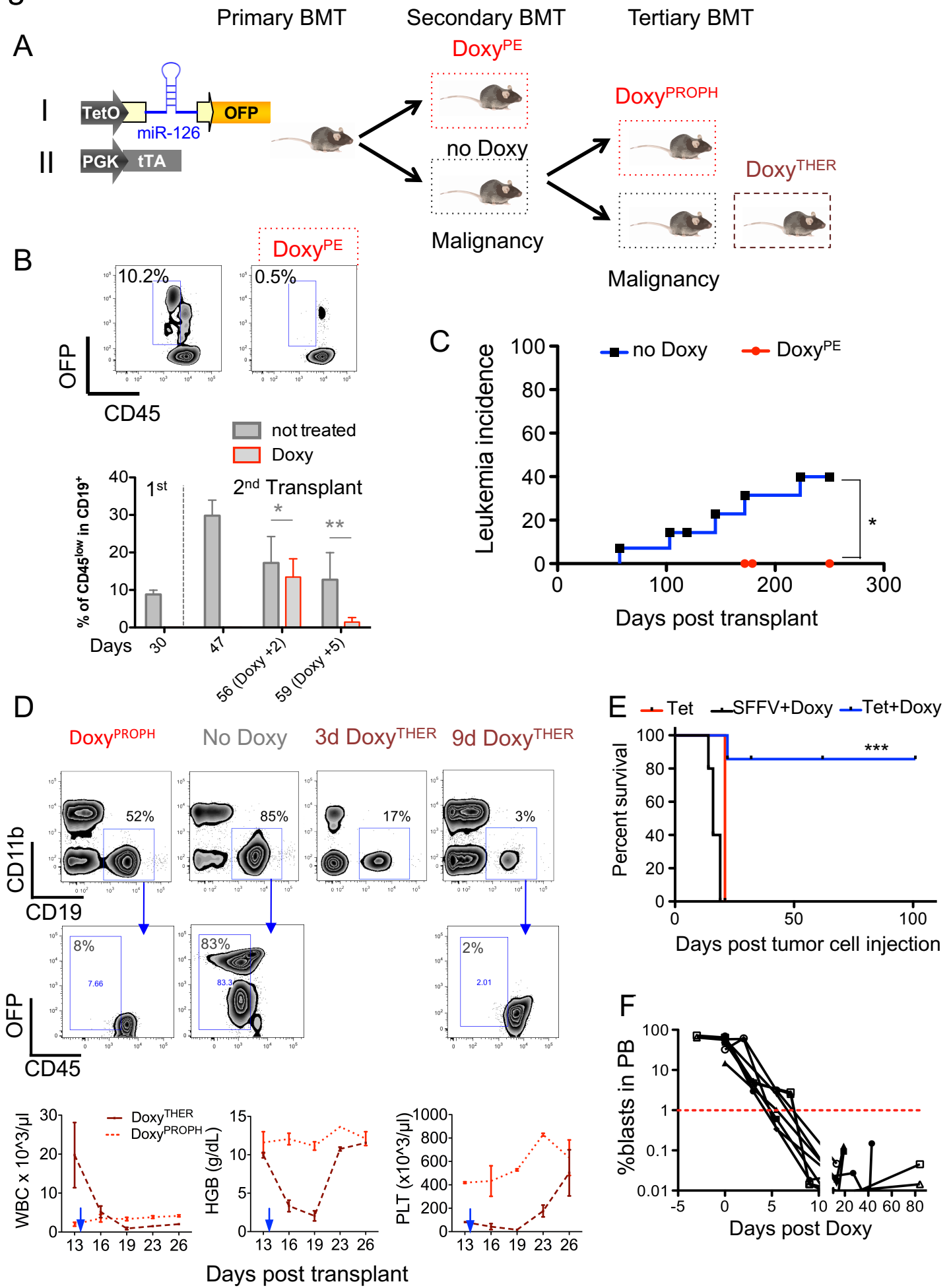
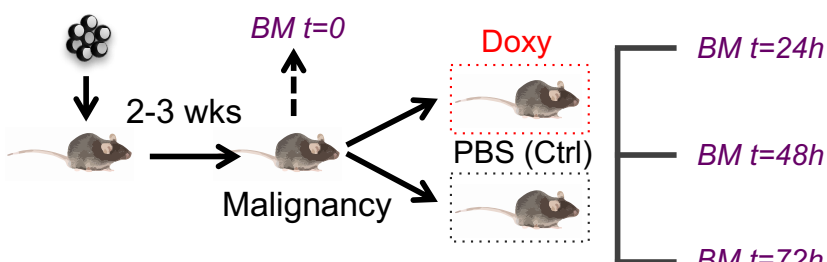
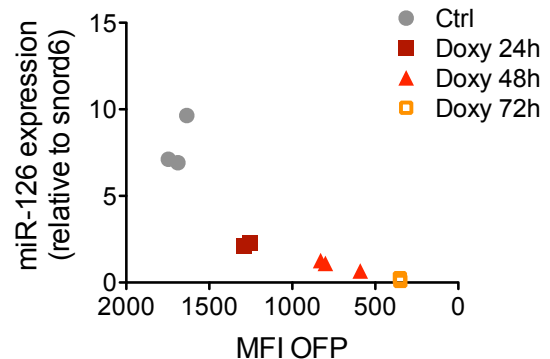


# Figure 3

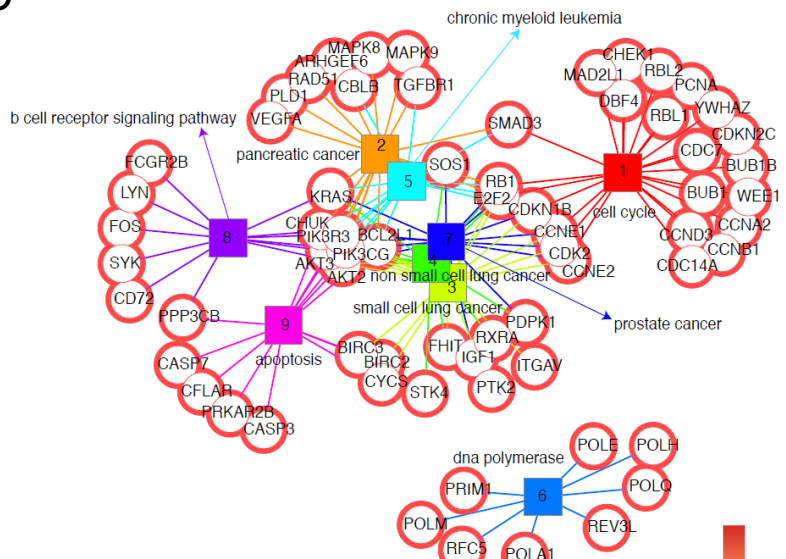
A



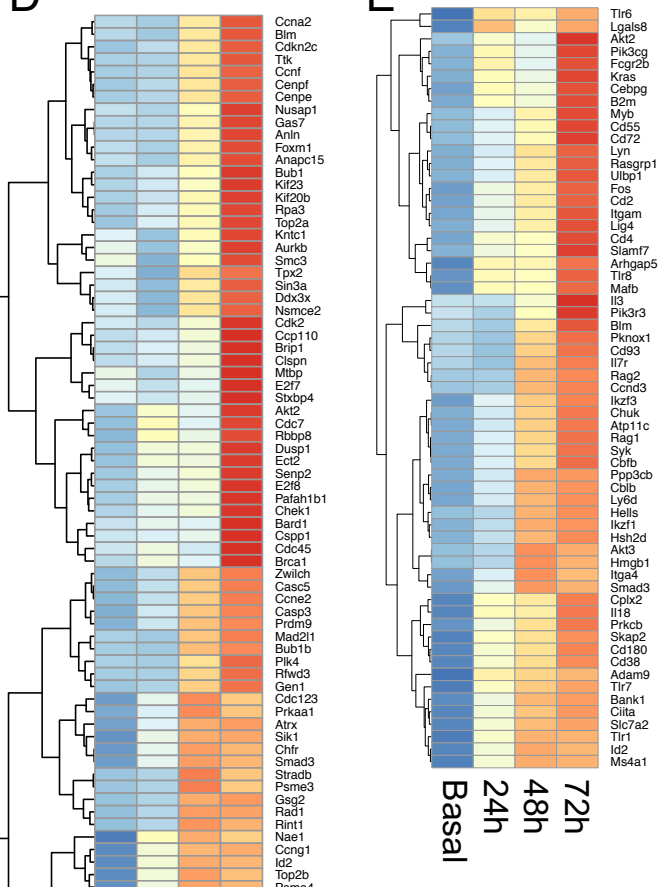
B



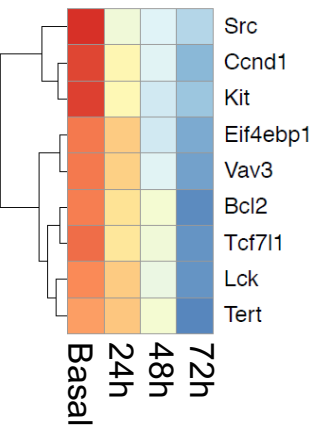
C



D



G



F

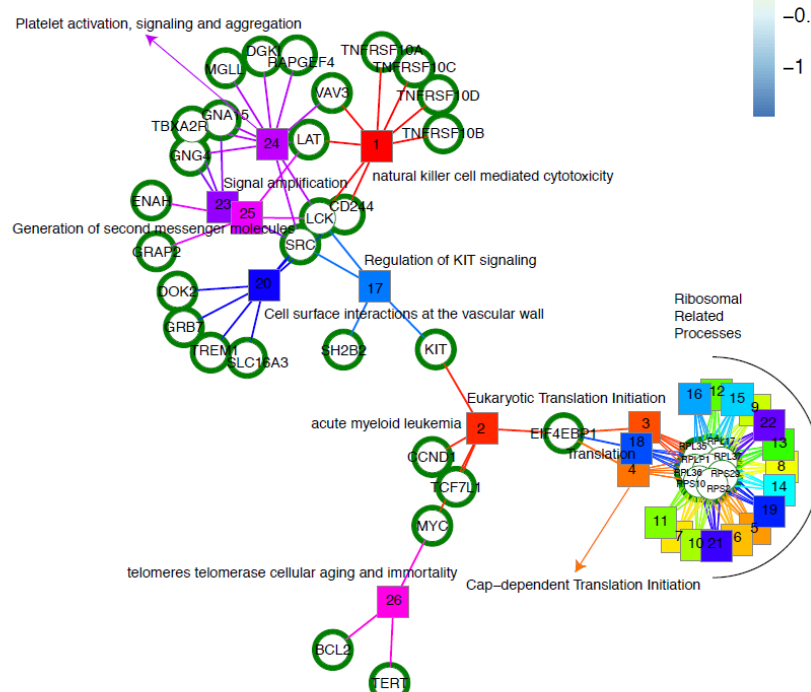


# Figure 4

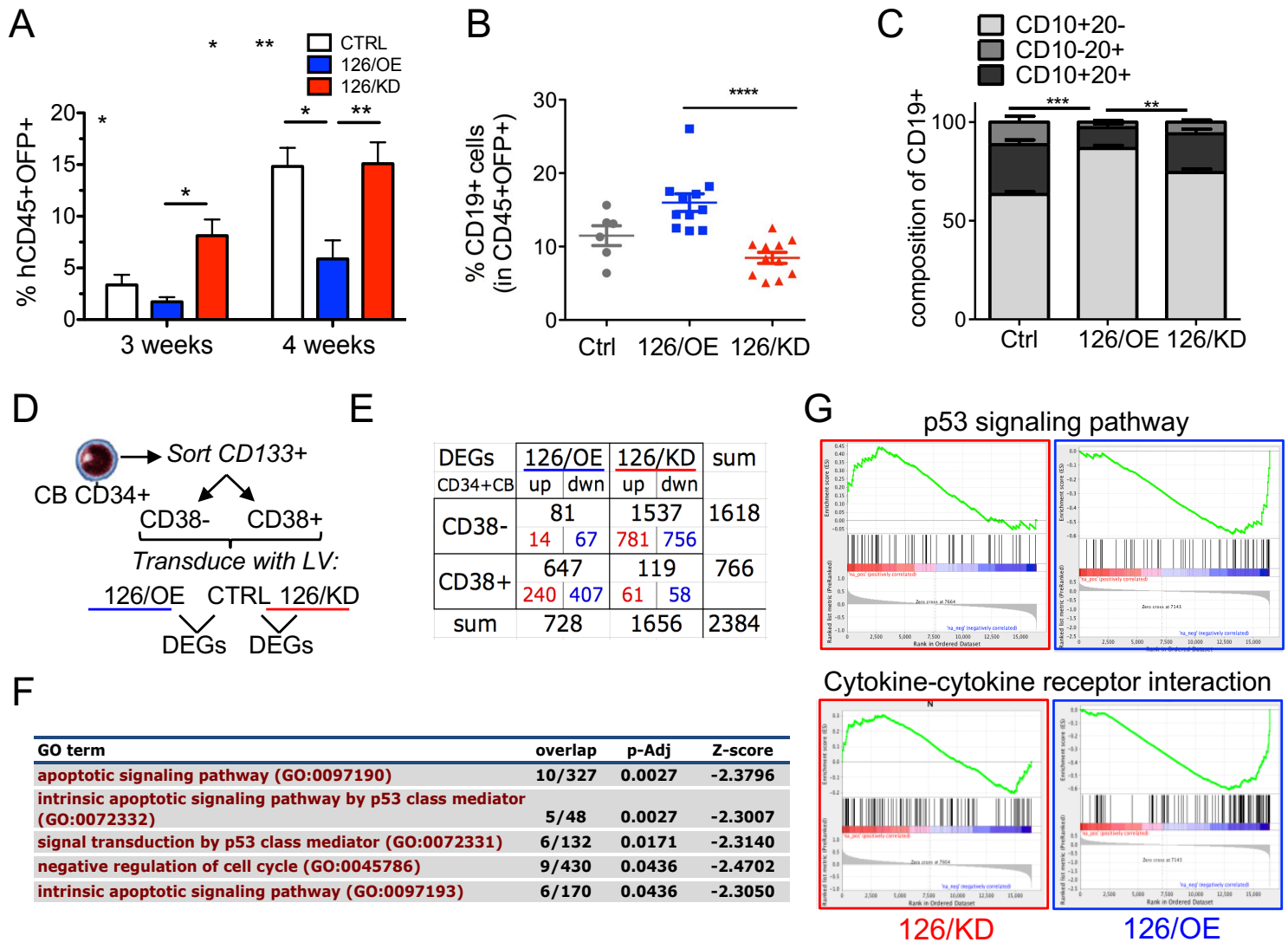


# Figure 5

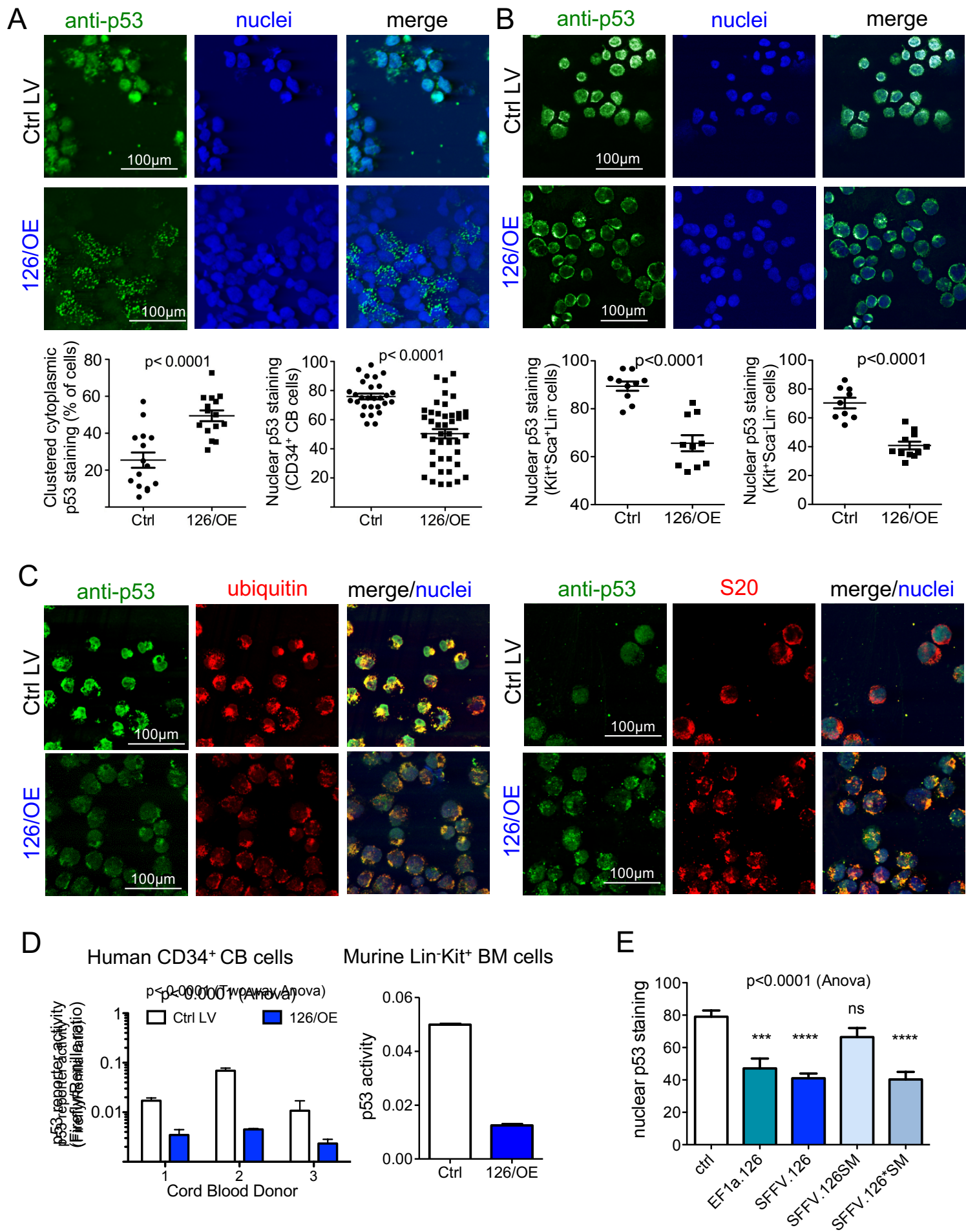
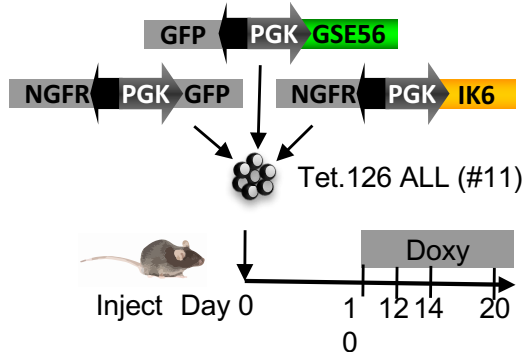
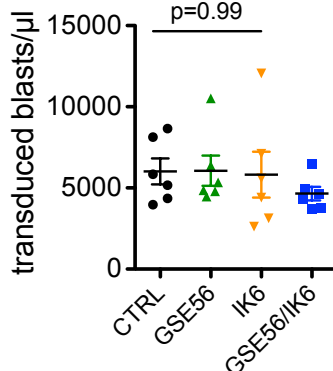


# Figure 6

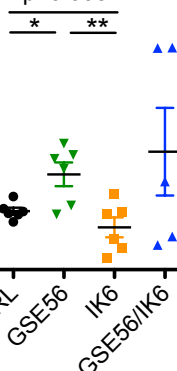
A



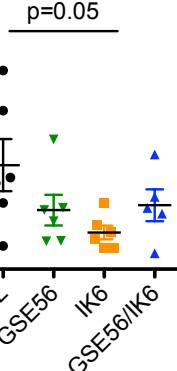
Day 10



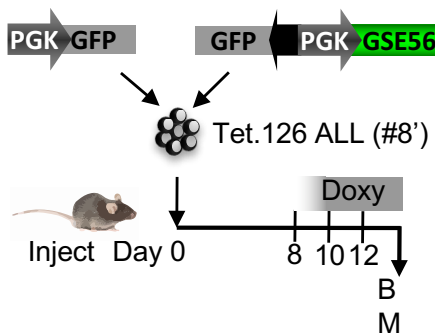
Day 12



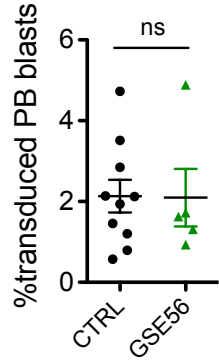
Day 14



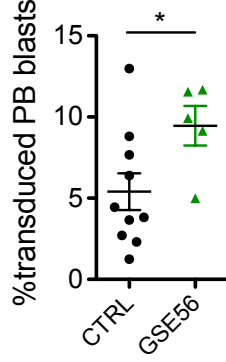
B



Day 10



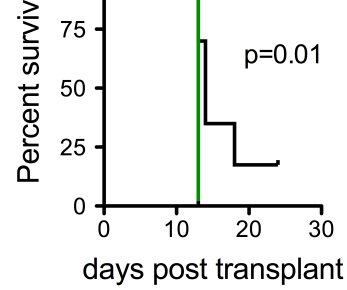
Day 12



— GSE56

— Ctrl

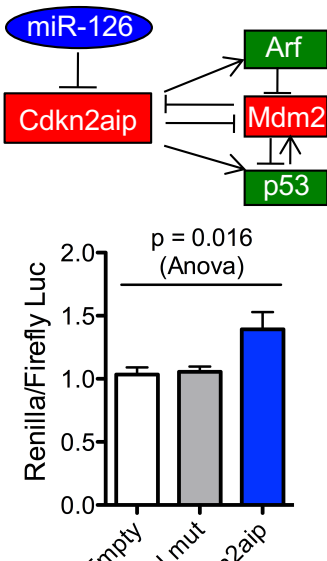
Percent survival



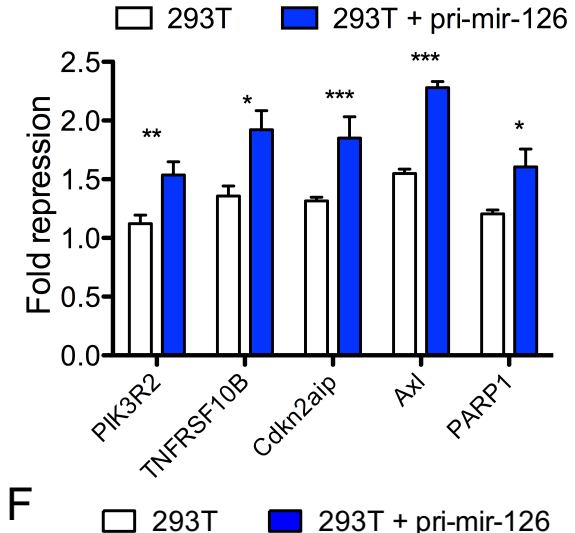
C

mu B-ALL	126-3p	126-5p
E2f7	3/5	4/5
Golp3	3/5	3/5
<b>Cdkn2aip</b>	3/5	2/5
<b>Spred1</b>	3/5	-
<b>Plk2</b>	3/5	-
<b>Vcam1</b>	3/5	-
<b>Axl</b>	3/5	-
Il10ra	3/5	-
Alg10b	3/5	-
Sgpp1	3/5	-
Sgpp1	3/5	-
Cdc14a	2/5	2/5
Rnf170	2/5	2/5
Gna13	2/5	-
0610010F05Rik	2/5	-
Tfb1m	2/5	-
Lnp	2/5	-
Rab43	2/5	-

D



E



—

—

293T + pri-mir-126

— 293T + pri-mir-126

—

—

—

293T + pri-mir-126

—

—

—

293T + pri-mir-126

—

—

—

293T + pri-mir-126

—

—

—

293T + pri-mir-126

—

—

—

293T + pri-mir-126

—

—

—

293T + pri-mir-126

—

—

—

293T + pri-mir-126

—

—

—

293T + pri-mir-126

—

—

—

293T + pri-mir-126

—

—

—

293T + pri-mir-126

—

—

—

293T + pri-mir-126

—

—

—

293T + pri-mir-126

—

—

—

293T + pri-mir-126

—

—

—

293T + pri-mir-126

—

—

—

293T + pri-mir-126

—

—

—

293T + pri-mir-126

—

—

—

293T + pri-mir-126

—

—

—

293T + pri-mir-126

—

—

—

293T + pri-mir-126

—

—

—

293T + pri-mir-126

—

—

—

293T + pri-mir-126

—

—

—

293T + pri-mir-126

—

—

—

293T + pri-mir-126

—

—

—

293T + pri-mir-126

—

—

—

293T + pri-mir-126

—

—

—

293T + pri-mir-126

—

—

—

293T + pri-mir-126

—

—

—

293T + pri-mir-126

—

—

—

293T + pri-mir-126

—

—

—

293T + pri-mir-126

—

—

—

293T + pri-mir-126

—

—

—

293T + pri-mir-126

—

—

—

293T + pri-mir-126

—

—

—

293T + pri-mir-126

—

—

—

293T + pri-mir-126

—

—

—

293T + pri-mir-126

—

—

—

293T + pri-mir-126

—

—

—

293T + pri-mir-126

—

—

—

293T + pri-mir-126

—

—

—

293T + pri-mir-126

—

—

—

293T + pri-mir-126

—

—

—

293T + pri-mir-126

—

—

—

293T + pri-mir-126

—

—

—

293T + pri-mir-126

—

—

—

293T + pri-mir-126

—

—

—

293T + pri-mir-126

—

—

—

293T + pri-mir-126

—

—

—

293T + pri-mir-126

—

—

—

293T + pri-mir-126

—

—

—

293T + pri-mir-126

—

—

—

293T + pri-mir-126

—

—

—

293T + pri-mir-126

—

—

—

293T + pri-mir-126

Figure 7

